small
NANO MICRO
www.small-journal.com

Bioinspired Universal Flexible Elastomer-Based Microchannels

*Feng Wu, Songyue Chen, Baiyi Chen, Miao Wang, Lingli Min, Jack Alvarenga, Jie Ju, Ali Khademhosseini, Yuxing Yao, Yu Shrike Zhang, Joanna Aizenberg, and Xu Hou**

Flexible and stretchable microscale fluidic devices have a broad range of potential applications, ranging from electronic wearable devices for convenient digital lifestyle to biomedical devices. However, simple ways to achieve stable flexible and stretchable fluidic microchannels with dynamic liquid transport have been challenging because every application for elastomeric microchannels is restricted by their complex fabrication process and limited material selection. Here, a universal strategy for building microfluidic devices that possess exceptionally stable and stretching properties is shown. The devices exhibit superior mechanical deformability, including high strain (967%) and recovery ability, where applications as both strain sensor and pressure-flow regulating device are demonstrated. Various microchannels are combined with organic, inorganic, and metallic materials as stable composite microfluidics. Furthermore, with surface chemical modification these stretchable microfluidic devices can also obtain antifouling property to suit for a broad range of industrial and biomedical applications.

Advances in microfluidics are revolutionizing many traditional disciplines, such as materials science,[1–4] molecular biology,[5–7] cellular biology,[8–12] drug screening,[3,13–17] and medical diagnostics.[18] Elastomeric microfluidics with rapid development in recent years has shown exciting potential from wearable electronic devices[19–22] for convenient digital lifestyle to biomedical devices[22–24] that make conformal interfaces with the skin and internal organs. However, their broad applications have been significantly restricted by the complex fabrication process[25,26] and the limited material selection.[27–29] For example, Ziegler et al. showed a classic and reproducible method to realize the fabrication of elastomeric microfluidics by micromolding and thermal bonding of Parylene.[28] Compared to the general fabrication method, where a sacrificial photoresist layer is sandwiched between two Parylene layers, the poisonous and high-residue photoresist dissolution step is omitted, and the adhesion between the elastomeric Parylene layers is improved. Nevertheless, the micromolding technique is complicated and expensive, which is difficult to adapt to industry requirements at present. In addition, Ota et al. developed a platform to conveniently fabricate liquid–liquid "heterojunction" devices for the use as liquid-state electronic elastomeric systems.[27] But this method has been significantly limited by its circumscribed material selection. Moreover, the inner surfaces of these microchannels are easily contaminated due to the strong adsorption of molecules onto these bulk materials.[30,31] The above-mentioned issues have largely affected the development of the conventional elastomeric microfluidic devices and their applications in various fields, such as wearable electronic devices,[1,19–22] biomolecule separation,[32,33] and antifouling technology.[30,31]

F. Wu, Dr. M. Wang, Prof. X. Hou
Bionic and Soft Matter Research Institute
College of Physical Science and Technology
Xiamen University
361005 Xiamen, China
E-mail: houx@xmu.edu.cn
Prof. S. Chen
Department of Mechanical and Electrical Engineering
Xiamen University
361005 Xiamen, China
Dr. B. Chen, Dr. L. Min, Prof. X. Hou
College of Chemistry and Chemical Engineering, and Collaborative Innovation Center of Chemistry for Energy Materials, and State Key Laboratory of Physical Chemistry of Solid Surfaces, and Pen-Tung Sah Institute of Micro-Nano Science and Technology
Xiamen University
361005 Xiamen, China
Dr. J. Alvarenga, Prof. A. Khademhosseini, Dr. Y. S. Zhang, Prof. J. Aizenberg
Wyss Institute for Biologically Inspired Engineering
Harvard University
Cambridge, MA 02138, USA
Dr. J. Ju, Prof. A. Khademhosseini, Dr. Y. S. Zhang
Biomaterials Innovation Research Center
Division of Engineering in Medicine
Department of Medicine
Brigham and Women's Hospital
Harvard Medical School
Cambridge, MA 02139, USA
Y. Yao, Prof. J. Aizenberg
Department of Chemistry and Chemical Biology
Harvard University
Cambridge, MA 02138, USA

DOI: 10.1002/smll.201702170

To overcome above challenges, various strategies have been proposed to prepare elastomeric microchannel (EM). Yuk et al. reported a method to assemble hydrogels and elastomers into hybrids with robust interface and functional microstructures, such as microchannels and electrical circuits inside hydrogels.[34] They used the double-sided acrylic tape elastomers which are made of mixtures of aliphatic acrylate photocured during the film processing (3M VHB membranes) as the good packaging material to seal the hydrogel. Besides, Kubo et al. described a strategy for fabricating the stretchable and mechanically stable radiofrequency antenna, which consisted of liquid metal enclosed in the elastomeric microfluidic channels.[35] Its high stretchability allowed its resonance to be mechanically tuned over a wide range of frequencies. To date, most of the elastomeric microfluidics that works under the conditions of the liquid is enclosed inside the channels without the flowing. Building elastomeric microfluidics with controllable channel sizes and dynamic flowing is still challenging due to material selection limitation, lack of simple and general fabrication process, and fouling issue, but has great potential applications, such as soft robotics[36] and tissue engineering.[37]

To address above issues, here we report a universal strategy to build bioinspired flexible elastomer-based microchannel systems with controllable channel sizes, which show extraordinarily stable and stretchable properties for many potential applications such as the strain sensor and the pressure-flow regulating device. Though showing the excellent flexibility and high adhesion, 3M VHB membrane has been applied in the large research and industrial communities only as the adhesive tapes. Here, we used 3M VHB membranes not only as the good packaging material but also as the important substrate for directly preparing the microchannels. And our microchannel fabrication is compatible with many existing techniques, such as laser cutting,[38] blade cutting,[39] photolithography,[40] and thermomolding,[41] and is also easily scalable for the large-scale fabrication. These stable elastomer-based microchannels not only exhibit excellent flexible and stretchable characteristics but also can show good antifouling property by further chemical modification of the inner surface of the channels. Such a universal approach for making dynamic microfluidics can potentially serve as a new platform with broad applications.[1]

Blood vessels in living organisms have multidimensional channels structures, with flexibility and stretchability.[42,43] Inspired by blood vessels, the multidimensional (1D, 2D, and 3D) microchannels were fabricated to show the flexible and stretchable properties (**Figure 1**a). For 1D, the EM possessed excellent flexibility and allowed the liquid flow inside the channel without any leakage even in a large-scale curve. For 2D, the EM patterned in alphabetic letters would be easily prepared by utilizing the laser cutting method (Figure 1a, bottom left and Figure S1, Supporting Information). These microchannels could be homogeneously fabricated, with size easily tuned by the laser power and the engraving time (Table S1 and Figures S2 and S3, Supporting Information). For 3D, the elastomer-based microchannels could be obtained by the stacking method, and tested with the external force applied. It showed the excellent sealability after stretching and releasing (Figure 1a, bottom right and Video S1, Supporting Information). The size of blood vessels in living organisms is controllable by blood pressure to maintain normal metabolism.[44,45] Our bioinspired microchannels could also regulate the channel size by controlling the flow pressure (Figure 1b).

One particularity of elastomer-based microchannels originates from its superelastic property. To further explore the mechanical property, tensile test was performed in comparison with the standard polydimethylsiloxane (PDMS) microchannel, as shown in **Figure 2**a. With the difference from PDMS, the EM sustained continuous spreading and demonstrated the superior stretchability, as well as the elastic-strain recovery ability after releasing (Video S2, Supporting Information). The stress–strain curves of both materials are shown in Figure 2b. The elongation of the

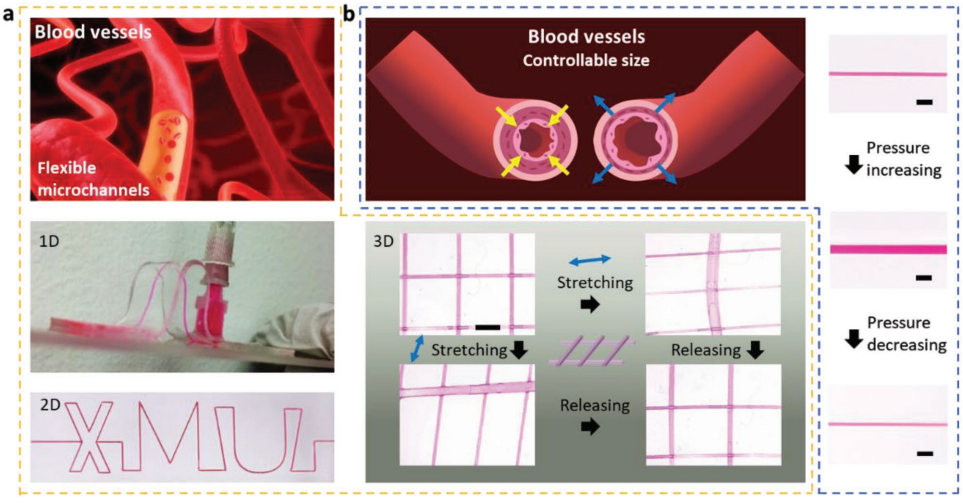

Figure 1. a) Bioinspired flexible microchannels. Flexible blood vessels (top left). 1D flexible elastomer-based microchannel (middle left), 2D elastomer-based microchannel with the letter pattern (bottom left), and 3D elastomer-based microchannels with stretchable and reversible properties (bottom right). Schematic adapted from the website at http://clipground.com/blood-vessels-clipart.html. b) Bioinspired microchannels with controllable sizes. Blood vessels with tunable sizes (top left). The size changes of the elastomer-based microchannel by regulating the flowing pressure (right). Scale bars, 2 mm.

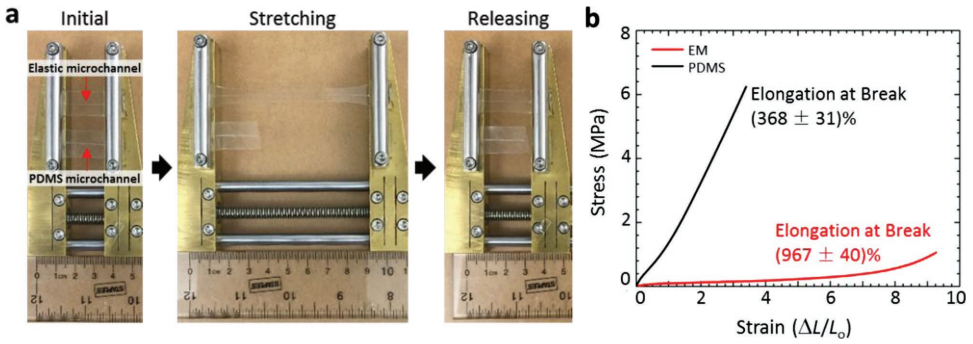

Figure 2. The mechanical property of the elastomeric stretchable microchannel. a) Comparative experiment between the EM and PDMS-based microchannel. b) Stress–strain curves of the EM and PDMS.

EM at break reached 967 ± 40%, compared with 368 ± 31% for that of PDMS. The Young's modulus of the EM calculated at linear deformation region reaches ≈60 kPa, which is a rather low value even for the elastic polymer materials.

A strain gauge was designed for the sensitive force sensing based on the outstanding mechanical property of the EM at small forces, as shown in **Figure 3**a. Resistance change of microchannel was measured under different tension. The microchannel was filled with 0.1 M KCl as the ionic conductor, and the current was measured by applying 0.1 V to two Ag/AgCl electrodes inserted into both the inlet and outlet. The ionic conductor in this microchannel served as the deformable interconnections without the risk of cracking as is the concern for metal interconnections.[46,47] The normalized resistance change $\Delta R/R$ is a function of strain s

$$\frac{\Delta R}{R} = \frac{1+s}{(1-\nu s)^2} - 1 \tag{1}$$

where $s = \Delta L/L_o$, and ν represents the Poisson's ratio for the microchannel. Figure 3b shows the normalized resistance change with respect to stress. The corresponding real-time current change measurement is shown in Figure S4a (Supporting Information). The measured Poisson's ratio of EM took the value of ≈0.15, while the fitting curve (Figure 3b inset) with the experimental data of ν for the microchannel was 0.093, indicating that compared with the bulk material, the microchannel has less transversal dimension change when being stretched. The strain gauge possesses a force sensitivity of $6\Delta R/R$ N^{-1}. Another potential advantage of the EM over PDMS for application in sensing lies in that the gas impermeability of the EM allows long-term chemical stability for the liquid filled inside the channel.[48,49]

Besides the longitude deformability, the fabricated microchannel device also showed the lateral deformability. The shape of the channel's cross section was recorded upon stretching the device and releasing. As shown in **Figure 4**a, the six-colored channels of triangular shape were discretely distributed. It should be noted that, there was no liquid inside the microchannels when we obtained the images of the cross section of these channels. Before we obtained these images, the inner wall of these microchannels had been dyed with the Rhodamine B solution, and then we dried it to obtain a clear contour of the channels when taking the images during its deformation. By applying an in-plane force perpendicular to the channels, the initial triangular channels completely closed and the section thickness decreased. After releasing the force, this highly compressed state completely recovered and the channels opened again owning to the excellent elastic property of EM.

The force-sensitive deforming feature of this elastomer-based microfluidic device showed great potential in the application of force/pressure regulation. Figure 4b has provided a simple illustration of such application. A syringe pump was used here to supply continuous fluid at a constant flow rate

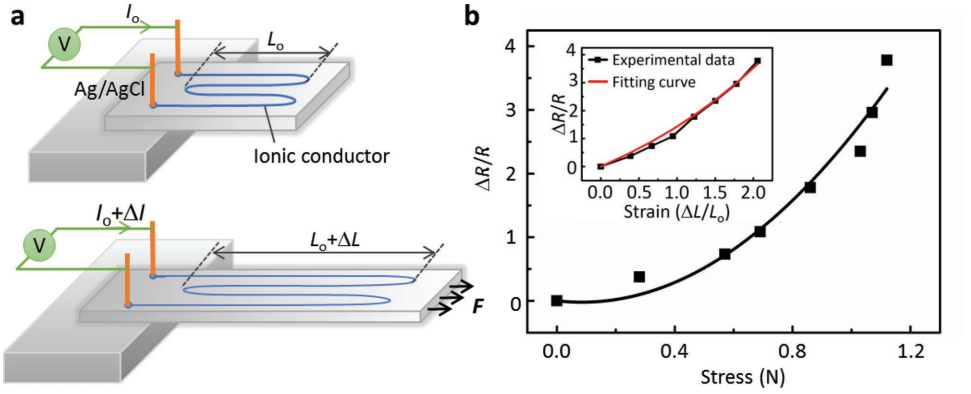

Figure 3. a) Strain gauge based on the EM and the ionic conductor. b) Resistance change curve with the different stress, where the inset is the normalized resistance change with the different strain.

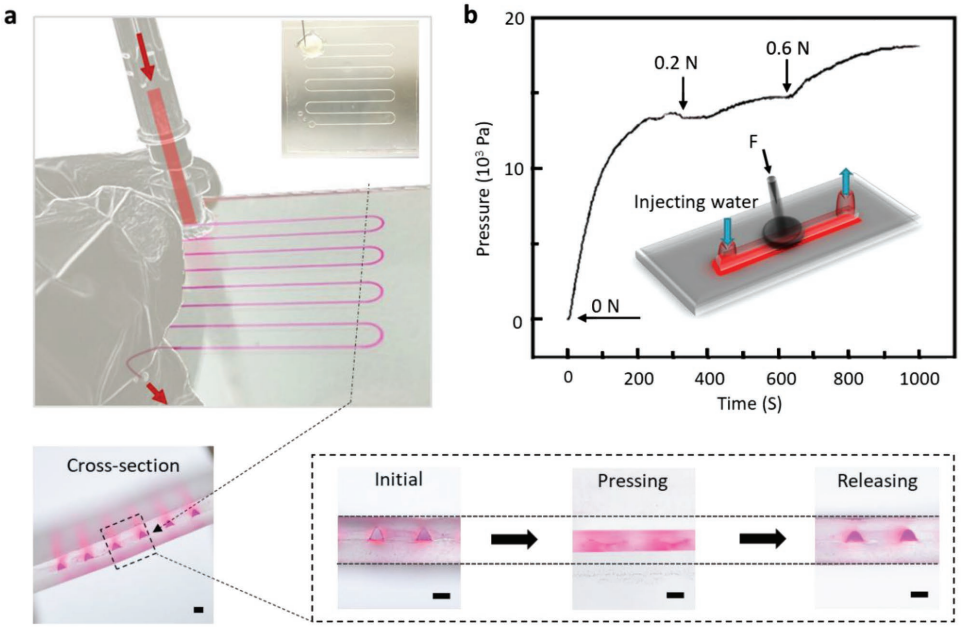

Figure 4. The elastomer-based microchannel's application as a pressure sensor. a) The compressible microchannels and its excellent recovery property. After crosscutting, separated microchannels can be observed clearly. By applying a force perpendicular to the channels, the initial triangular microchannels completely closed and the section thickness decreased. After releasing, the closed microchannels fully recovered again. Inset image shows a clear microfluidics before injection. b) Applied forces can be reflected by the variation of the transfer liquid pressure inside the microchannel. Scale bars, 400 μm.

Q (300 μL min^{-1}) into a single-channeled microfluidic device and a digital cantilever capable of supplying small amount of force was harnessed to exert force to the upper surface of the microchannel. A highly sensitive pressure gauge connected near the inlet and outlet of the channel was used to monitor the real-time pressure change. The pressure drop $\Delta P = Q \cdot R_{hyd}$, where flow rate $Q \approx v_s \cdot w \cdot h$, the hydraulic resistance $R_{hyd} \approx \alpha \mu L / w h^3$, and v_s denotes the fluid velocity, μ the viscosity of the fluid, L, w, and h the length, width, and height of the channel for the rectangular cross section, respectively, and α the constant related to the shape of the cross section.[50,51] Therefore, for the constant flow rate in our case, ΔP is inversely proportional to h^2. The cross-section size is reduced by pressing on the microchannel, causing the increase of the hydraulic resistance and finally pressure boosting.

Specific to the experiment, the initial size of the channel without any pressure was ≈250 μm in width, and ≈400 μm in height and the velocity of water was set to be 300 μL min^{-1}. In the first 200 s, the pressure was building up to a relatively stable value of 13 kPa without external force to the upper surface. At 400 s, the force of 0.2 N was exerted to the exterior surface of the channel, ΔP increased accordingly and stabilized at about 11.3 kPa at 600 s. After that, the force was elevated to 0.6 N, and ΔP underwent another climbing to 18 kPa at 1000 s. For a microfluidic system with fixed diameter and inner fluid velocity, the force can be detected by using the force–pressure drop calibration curve, indicating a potential application for the pressure sensor system.

Another superiority of this microfluidics was its vast applicability on various substrates directly, without any surface modifications. As illustrated in **Figure 5**, due to its intrinsic adhesive property, the EM could be transferred on various substrates, including organic (polyethylene terephthalate (PET), polytetrafluoroethylene (PTFE), PDMS, and polymethyl methacrylate (PMMA)), inorganic (glass), and metallic materials. The EM adhered firmly onto different types of substrates, and did not show any leakage from the magnified images. For the metal EM, the seal of the channel was intact even after severe bending. The 90° peeling test and the liquid-leakage critical pressure measurement also showed good sealing property (Figure S5, Supporting Information).

Fouling is a daunting issue[30] and restricts practical applications of microfluidic channels. To avoid fouling, we modified the inner surface of the microchannel with the amphiphobic agent 1H,1H,2H,2H-perfluorodecyltrimethoxysilane (PFTS) by using the chemical vapor deposition method. As can be observed in **Figure 6**, the evident changes in the wettability and the antifouling capacity of the EM occurred in the process of modification. In Figure 6a, water and dimethylsilicone oil were tested as representative chemicals, where the contact angle analysis was used to test the modification. The inner surface of the microchannel without any treatment showed the contact angles of 82.3° to water droplet and 9.7° to dimethylsilicone oil, respectively, indicating an amphipathicity of the EM. However, after modification by PFTS, the remarkable changes took place in the wettability of the EM surface. As shown in Figure 6a, the intrinsic hydrophilicity transformed into hydrophobic (the contact angle of water increased from 82.3° to 118.8°) and the contact angle of dimethylsilicone oil significantly increased from 9.7° to 72.2°. Meanwhile, the PFTS coating exhibited an excellent antifouling capacity. As shown in Figure 6b, the

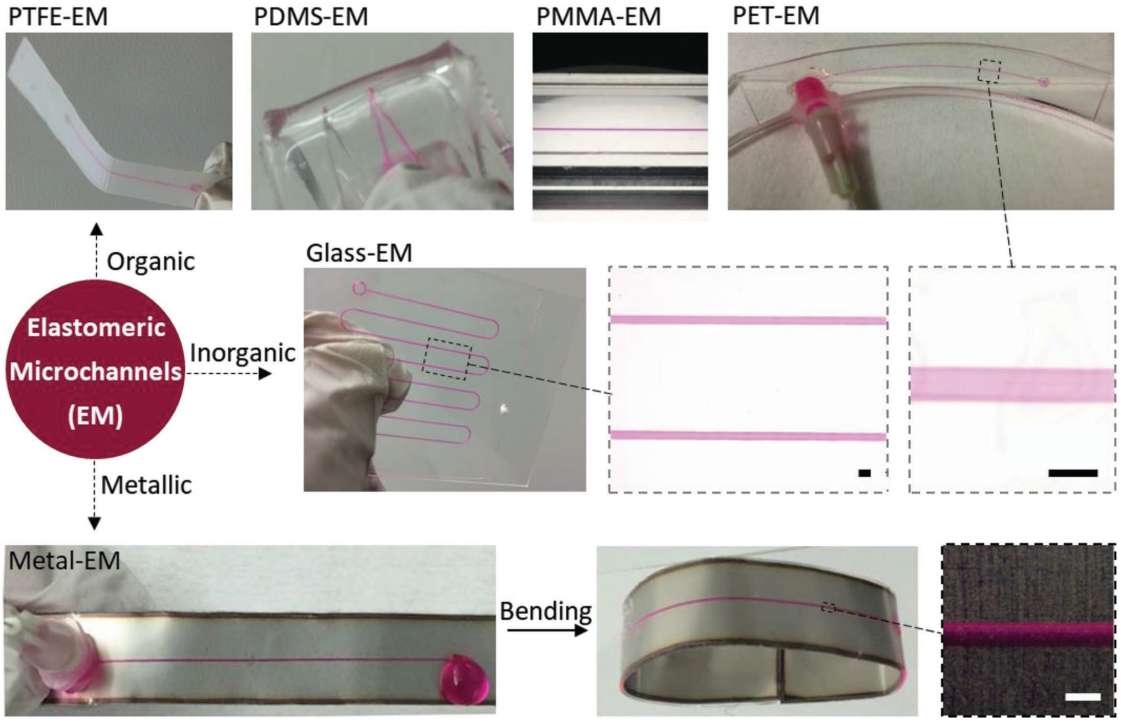

Figure 5. The composite microfluidics prepared by combining the EM with the organic polymeric substrates, the inorganic glass substrate, and the metallic substrate. Scale bars, 200 µm.

modified microchannel inner surface could completely recover to its initial state without any residue of Rhodamine B, while the microchannel without modification showed the serious contamination with the dye molecules. It should be noted that, the surface could also be modified with many other different methods to suite different applications, such as the liquid phase deposition[52] and the chemical composition.[53]

In summary, we have demonstrated a convenient method to fabricate the elastomer-based microchannel, which possesses the excellent elastic property and dynamic stability with maintaining liquid flows during the stretching and releasing state. Meanwhile, the flexible microchannel can be directly assembled onto various substrates, including organic, inorganic, and metallic. Besides, its inner surface can be conveniently

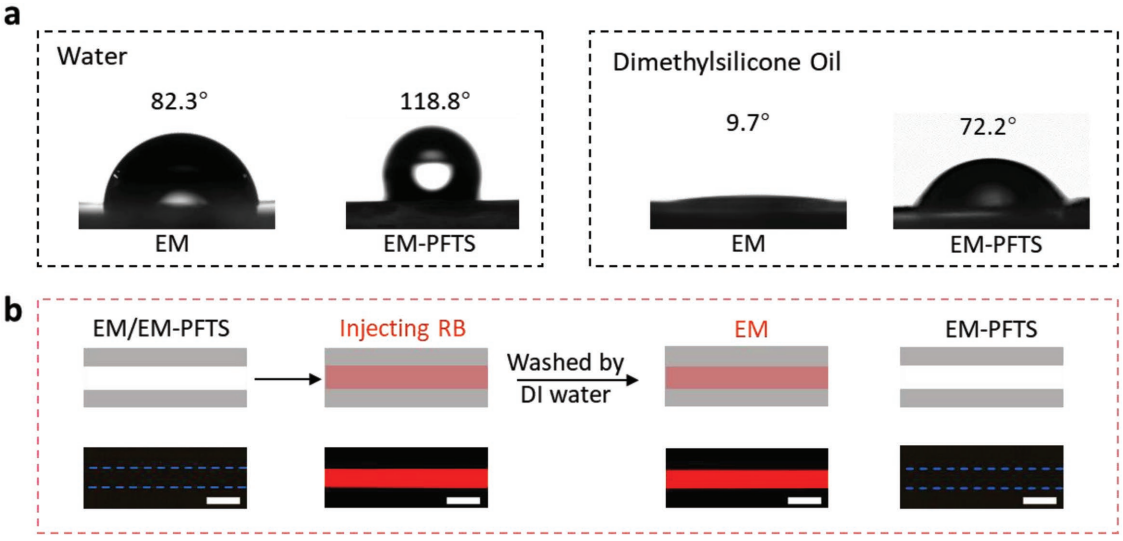

Figure 6. Surface modification of the microchannel inner surface for antifouling. a) Water and dimethylsilicone oil contact angle analysis. b) Schematic illustrations (top) and microscopic images of microchannels (bottom). Antifouling measurement before and after the surface modification with PFTS on the microchannel inner surface. Scale bars, 50 µm.

modified by a simple chemical vapor deposition method for antifouling application. In addition, the elastomer-based microchannel exhibits excellent mechanical deformability upon stretching (967%) and compressing. Meanwhile, its sensitive deformability upon microforces, including both in longitude and lateral directions, shows great potential in the application for strain sensors and pressure sensors.

Experimental Section

For the microchannels materials, the elastomer (VHB 4910, 3M Company) and PDMS (Sylgard 184, Dow Corning Corporation) with the ratio of base:cross-linker 10:1 were used. To prevent fouling, PTFE (J&K Chemicals, 227930) was used to modify the microchannel inner surface. Both the deionized (DI) water (resistivity = 18.3 MΩ cm) and the dimethylsilicone oil (Macklin, D806810) were used to characterize the wetting behavior of the material surface. KCl (Sinopharm, 10016308) was used to act as the ionic conductor. For the antifouling measurement, Rhodamine B (Sigma-Aldrich R6626) was used.

Fabrication of Microchannels: The flexible and PDMS microchannels were fabricated by cutting the channel directly with versalaser cutting engraving system (GCC, Spirit SI-25), at the power of 50 W and cutting speed of 10 mm s^{-1}. The resolution of this system is 1500 PPI. The flexible 3D microchannels had two layers. Structures were made both inside the two layers of the VHB tapes, then adhered together to fabricate 3D microchannels as shown in Figure 1a.

Mechanical Testing: The EM and PDMS microchannels maintained consistent properties over the time of the tests. All microfluidic devices were prepared with 1.5 cm in width, 2.5 cm in length, and 2 mm in thickness. The size of channels was ≈250 µm in width and ≈400 µm in height. A homemade device was used to test the stretching ability of both EM and PDMS elastomers as shown in Figure 2. Screw tightened bars were utilized to stabilize both ends of samples. Constant tension of the sample could be finely controlled by the device. All tests were performed in ambient air at room temperature.

Strain Gauge: After the flexible microchannel pattern with 2 cm in length, 1.5 cm in width, and 2 mm in thickness was prepared following the above-mentioned method, the microchannel was filled with 0.1 M KCl as the ionic conductor. The current was measured while inserting two Ag/AgCl electrodes into the inlet and outlet of the clip. A voltage of 0.1 V was applied by Keithley 2400 source meter. The sensing test was performed by stretching from relaxing length of 2–5.5 cm.

Pressure Measurements: A syringe pump was used to supply continuous fluid at a constant flow rate Q (300 mL min^{-1}) in a single-channeled microfluidics with ≈250 µm in width and ≈400 µm in height. A digital cantilever capable of supplying small amount of force was harnessed to exert force to the upside surface of the microchannel. A pressure gauge, pressure transmitter (PX273-030DI) from Omega, connected near the inlet and outlet of the channel was used to monitor the real-time pressure change, during flow of deionized water as shown in Figure 4.

Peeling Test: All substrates were prepared with 2 cm in width, 3 cm in length, and 1 mm in thickness. The EM was adhered onto various substrates. The samples were tested with a constant 90° peeling (Instron 5948 microtester) speed of 10 mm min^{-1}. Steady state of peeling force was finally measured in this process.

Liquid-Leakage Critical Pressure Measurement: The critical pressure was measured following the method mentioned in the Pressure Measurements section. The size of channels was ≈270 µm in width and ≈500 µm in height.

Contact Angle Measurements: The contact angle was measured with a contact angle measurement system (OCA100, Dataphysics) at room temperature. A droplet of 5 µL, either water or dimethylsilicone oil, was placed on the surface of the sample and the droplet profile was captured. For each sample, a mean value of the contact angle was calculated from at least three individual measurements taken at different locations on the examined samples.

Surface Modification for Antifouling: The microchannel was modified by PFTS to obtain the antifouling capacity. The size of channels is ≈250 µm in width and ≈400 µm in height. The exposed microchannel inner surface without any treatment was placed in a desiccator together with an open glass dish containing about 0.5 mL of PFTS. Subsequently, the desiccator was closed again and chemical vapor deposition of silane was carried out for 3 h under 80 °C. The inner surfaces finally achieved the antifouling capacity, and then the two pieces of modified the EM were adhered to form the microfluidic channel. For comparison, an unmodified microfluidic device was also prepared, and these two microfluidic devices were both injected with the Rhodamine B aqueous solution. The Rhodamine B aqueous solution used in the microfluidic experiments was prepared by dissolving Rhodamine B in DI water to give a final concentration of 0.1 mg mL^{-1}. After injecting the Rhodamine B solution into the unmodified/modified microfluidic for 5 s, DI water was injected to wash the channels for 30 s. During this process, optical microscopy (Leica, DM6000B) was used to observed the fluorescence.

Supporting Information

Supporting Information is available from the Wiley Online Library or from the author.

Acknowledgements

F.W., S.C., and B.C. contributed equally to this work. This work was supported by the National Natural Science Foundation of China (No. 21673197), Young Overseas High-level Talents Introduction Plan, the 111 Project (No. B16029), and the Fundamental Research Funds for the Central Universities of China (No. 20720170050). J.A. acknowledges the Department of Energy under Award No. DE-SC0005247 and the Advanced Research Projects Agency-Energy (ARPA-E), U.S. Department of Energy, under Award No. DE-AR0000326. Y.S.Z. acknowledges the National Cancer Institute of the National Institutes of Health Pathway to Independence Award (K99CA201603), the Lush Prize, and the Science and Technology Commission of Shanghai Municipality (STCSM) 17JC 1400200. The authors thank M. Eggersdorfer, H. Meng, and Y. Fan for discussion and help.

Conflict of Interest

The authors declare no conflict of interest.

Keywords

bioinspired devices, elastomers, flexible microchannels

Received: June 26, 2017
Revised: September 27, 2017
Published online:

[1] X. Hou, Y. S. Zhang, G. Trujillo-de Santiago, M. M. Alvarez, J. Ribas, S. J. Jonas, P. S. Weiss, A. M. Andrews, J. Aizenberg, A. Khademhosseini, *Nat. Rev. Mater.* **2017**, *2*, 17016.
[2] E. K. Sackmann, A. L. Fulton, D. J. Beebe, *Nature* **2014**, *507*, 181.
[3] J. Clayton, *Nat. Methods* **2005**, *2*, 621.
[4] D. Psaltis, S. R. Quake, C. Yang, *Nature* **2006**, *442*, 381.
[5] T. A. Duncombe, A. M. Tentori, A. E. Herr, *Nat. Rev. Mol. Cell Biol.* **2015**, *16*, 554.

[6] G. M. Whitesides, *Nature* **2006**, *442*, 368.
[7] Y. Xu, M. Shinomiya, A. Harada, *Adv. Mater.* **2016**, *28*, 2209.
[8] B. Xiong, K. Ren, Y. Shu, Y. Chen, B. Shen, H. Wu, *Adv. Mater.* **2014**, *26*, 5525.
[9] D. Kim, X. Wu, A. T. Young, C. L. Haynes, *Acc. Chem. Res.* **2014**, *47*, 1165.
[10] Y. Cheng, F. Zheng, J. Lu, L. Shang, Z. Xie, Y. Zhao, Y. Chen, Z. Gu, *Adv. Mater.* **2014**, *26*, 5184.
[11] Y. S. Zhang, A. Khademhosseini, *Science* **2017**, *356*, 3627.
[12] S. Cheng, Y. Jin, N. Wang, F. Cao, W. Zhang, W. Bai, W. Zheng, X. Jiang, *Adv. Mater.* **2017**, *29*, 1700171.
[13] S. Xiao, J. R. Coppeta, H. B. Rogers, B. C. Isenberg, J. Zhu, S. A. Olalekan, K. E. McKinnon, D. Dokic, A. S. Rashedi, D. J. Haisenleder, *Nat. Commun.* **2017**, *8*, 14584.
[14] R. C. R. Wootton, A. J. Demello, *Nature* **2012**, *483*, 43.
[15] A. Albanese, A. K. Lam, E. A. Sykes, J. V. Rocheleau, W. C. W. Chan, *Nat. Commun.* **2013**, *4*, 2718.
[16] P. M. Valencia, O. C. Farokhzad, R. Karnik, R. Langer, *Nat. Nanotechnol.* **2012**, *7*, 623.
[17] P. Mitchell, *Nat. Biotechnol.* **2001**, *19*, 717.
[18] P. Yager, T. Edwards, E. Fu, K. Helton, K. Nelson, M. R. Tam, B. H. Weigl, *Nature* **2006**, *442*, 412.
[19] M. Kaltenbrunner, T. Sekitani, J. Reeder, T. Yokota, K. Kuribara, T. Tokuhara, M. Drack, R. Schwödiauer, I. Graz, S. Bauer-Gogonea, *Nature* **2013**, *499*, 458.
[20] S. Xu, Y. Zhang, L. Jia, K. E. Mathewson, K. I. Jang, J. Kim, H. Fu, X. Huang, P. Chava, R. Wang, *Science* **2014**, *344*, 70.
[21] J. C. Yeo, J. Yu, K. P. Loh, Z. Wang, C. T. Lim, *ACS Sens.* **2016**, *1*, 543.
[22] X. Pu, M. Liu, X. Chen, J. Sun, C. Du, Y. Zhang, J. Zhai, W. Hu, Z. Wang, *Sci. Adv.* **2017**, *3*, e1700015.
[23] A. Chortos, J. Liu, Z. Bao, *Nat. Mater.* **2016**, *15*, 937.
[24] J. Kim, M. Lee, H. J. Shim, R. Ghaffari, H. R. Cho, D. Son, Y. H. Jung, S. Min, C. Choi, S. Jung, *Nat. Commun.* **2014**, *5*, 5747.
[25] D. Qin, Y. Xia, G. M. Whitesides, *Nat. Protoc.* **2010**, *5*, 491.
[26] M. K. Verma, A. Majumder, A. Ghatak, *Langmuir* **2006**, *22*, 10291.
[27] H. Ota, K. Chen, Y. Lin, D. Kiriya, H. Shiraki, Z. Yu, T. J. Ha, A. Javey, *Nat. Commun.* **2014**, *5*, 5032.
[28] D. Ziegler, T. Suzuki, S. Takeuchi, *J. Microelectromech. Syst.* **2006**, *15*, 1477.
[29] S. Metz, R. Holzer, P. Renaud, *Lab Chip* **2001**, *1*, 29.
[30] R. Mukhopadhyay, *Anal. Chem.* **2005**, *77*, 429.
[31] K. J. Regehr, M. Domenech, J. T. Koepsel, K. C. Carver, S. J. Ellison-Zelski, W. L. Murphy, L. A. Schuler, E. T. Alarid, D. J. Beebe, *Lab Chip* **2009**, *9*, 2132.
[32] S. Marre, Y. Roig, C. Aymonier, *J. Supercrit. Fluids* **2012**, *66*, 251.
[33] N. Kockmann, J. Kastner, P. Woias, *Chem. Eng. J.* **2008**, *135*, S110.
[34] H. Yuk, Z. Teng, G. A. Parada, X. Liu, X. Zhao, *Nat. Commun.* **2016**, *7*, 12028.
[35] M. Kubo, X. Li, C. Kim, M. Hashimoto, B. J. Wiley, D. Ham, G. M. Whitesides, *Adv. Mater.* **2010**, *22*, 2749.
[36] S. A. Morin, G. M. Whitesides, *Science* **2012**, *337*, 828.
[37] I. Wagner, E. M. Materne, S. Brincker, U. Süssbier, C. Frädrich, M. Busek, F. Sonntag, D. A. Sakharov, E. V. Trushkin, A. G. Tonevitsky, *Lab Chip* **2013**, *13*, 3538.
[38] D. Snakenborg, H. Klank, J. P. Kutter, *J. Micromech. Microeng.* **2003**, *14*, 182.
[39] F. Cortés-Salazar, M. Träuble, F. Li, J. M. Busnel, A. L. Gassner, M. Hojeij, G. Wittstock, H. H. Girault, *Anal. Chem.* **2009**, *81*, 6889.
[40] J. R. Anderson, D. T. Chiu, H. Wu, O. Schueller, G. M. Whitesides, *Electrophoresis* **2000**, *21*, 27.
[41] K. Ren, W. Dai, J. Zhou, J. Su, H. Wu, *Proc. Natl. Acad. Sci. USA* **2011**, *108*, 8162.
[42] A. C. Burton, *Am. J. Physiol.* **1951**, *164*, 319.
[43] W. Wu, A. Deconinck, J. A. Lewis, *Adv. Mater.* **2011**, *23*, 178.
[44] B. Yuan, Y. Jin, Y. Sun, D. Wang, J. Sun, Z. Wang, W. Zhang, X. Jiang, *Adv. Mater.* **2012**, *24*, 890.
[45] P. Gong, W. Zheng, Z. Huang, W. Zhang, D. Xiao, X. Jiang, *Adv. Funct. Mater.* **2013**, *23*, 42.
[46] J. Lee, J. Wu, M. Shi, J. Yoon, S. Park, M. Li, Z. Liu, Y. Huang, J. A. Rogers, *Adv. Mater.* **2011**, *23*, 986.
[47] Y. Su, X. Ping, K. J. Yu, J. W. Lee, J. A. Fan, B. Wang, M. Li, R. Li, D. V. Harburg, Y. Huang, *Adv. Mater.* **2017**, *29*, 1604989.
[48] K. Ren, Y. Chen, H. Wu, *Curr. Opin. Chem. Biol.* **2014**, *25*, 78.
[49] P. L. Floch, X. Yao, Q. Liu, Z. Wang, G. Nian, Y. Sun, L. Jia, Z. Suo, *ACS Appl. Mater. Interfaces* **2017**, *9*, 25542.
[50] C. J. Morris, F. K. Forster, *Exp. Fluids* **2004**, *36*, 928.
[51] M. J. Fuerstman, A. Lai, M. E. Thurlow, S. S. Shevkoplyas, H. A. Stone, G. M. Whitesides, *Lab Chip* **2007**, *7*, 1479.
[52] M. Y. Liu, H. Wang, Y. Wang, *AIChE J.* **2010**, *53*, 1075.
[53] A. R. Statz, R. J. Meagher, A. A. E. Barron, P. B. Messersmith, *J. Am. Chem. Soc.* **2005**, *127*, 7972.

